Adaptive correction of a tightly focused, high-intensity laser beam by use of a third-harmonic signal generated at an interface

T. A. Planchon, W. Amir, J. J. Field, C. G. Durfee, and J. A. Squier
Colorado School of Mines, Golden, Colorado, 80401

P. Rousseau
Center for Ultrafast Optical Science, Ann Arbor, Michigan, 48105

O. Albert and G. Mourou
Laboratoire d'Optique Appliquée, ENSTA, Ecole Polytechnique, Paris, France

Received March 29, 2006; accepted April 26, 2006; posted May 10, 2006 (Doc. ID 69463)

By using the third-harmonic signal generated at an air–dielectric interface, we demonstrate a novel way of correcting wavefront aberrations induced by high-numerical-aperture optics. The third harmonic is used as the input physical parameter of a genetic algorithm working in closed loop with a 37-actuator deformable mirror. This method is simple and reliable and can be used to correct aberrations of tightly focused beams, a regime where other methods have limitations. Improvement of the third-harmonic signal generated with an $f/1.2$ parabolic mirror by 1 order of magnitude is demonstrated. © 2006 Optical Society of America

OCIS codes: 010.1080, 320.7090, 140.3590.

Tight focusing is one way to produce an ultrahigh laser intensity for high-field physics without increasing the laser energy. Adaptive optical correction of the wavefront is often necessary to produce a diffraction-limited focus[1] to compensate for wavefront aberrations in the amplified beam as well as aberrations from an imperfect focusing optic. As described below, the most important part of wavefront correction is obtaining a reliable error signal. Previously demonstrated methods of wavefront correction encounter several limitations when used in conjunction with high-numerical-aperture (NA) optics. We demonstrate in this Letter an unambiguous way to correct the focal spot of a tightly focused laser beam by using feedback from a readily available nonlinear optical signal. Our method involves the straightforward optimization of the third-harmonic signal generated from the interface of a simple glass slide placed at the focus. The third harmonic generated in this way has been used at NAs as high as 1.4 and over a wavelength from 800 nm to 1.5 μm.[2,3] The combination of these three parameters (a broad bandwidth, a signal efficiently produced in a tight focus, and simple, readily available nonlinear media) make the third-harmonic process an optimal marker for wavefront correction with ultrashort pulses focused at high NAs.

The most common method of correction of a laser wavefront is within a closed loop, where the wavefront aberrations are measured by a wavefront sensor and then corrected with an active optic.[1,4–7] There are several different factors that must be considered when assessing the accuracy of this method. First, the measured wavefront can be different from the wavefront of the focused beam. When the wavefront is measured *before* the focusing optic,[5,6] additional aberrations created by the final focusing optic are not corrected, while the optics in the wavefront measurement line itself can introduce aberrations that are not present in the beam. When the wavefront is measured *after* the focus,[1,4–7] high-NA optics that collect the light after the focus can also introduce aberrations due to their optical quality and alignment. Second, the wavefront measurement itself does not give information in the wings of the spatial profile where the number of photons is low; so wavefront correction will not be achieved across the whole beam.

The second method for correcting wavefront aberrations is the use of a physical parameter produced by the intense laser beam and an algorithm driving the active optics to optimize this parameter. Second-harmonic generation produced by a nonlinear crystal such as a thin β-barium borate crystal has been demonstrated.[8] A stronger nonlinear signal generated at the focus would correspond to a smaller focal spot. One important consideration in this method is the phase-matching angular acceptance of the nonlinear crystal. High-order harmonic generation (HHG) has also been used as the physical parameter to optimize at focus.[9,10] However, HHG implies a complicated experimental setup and is inefficient with high-NA optics, as a long Rayleigh range is needed to produce HHG. Moreover, some experimental results[9,10] do not agree on the wavefront shape that optimizes the HHG.

The third-harmonic signal produced at an interface gives an unambiguous merit signal for optimization and is simple to implement while being unrestricted by phase-matching considerations. A strong third-harmonic generation (THG) signal produced when an intense short laser pulse is tightly focused at an air–dielectric interface was demonstrated by Tsang.[11] At the interface the inversion symmetry of the bulk is broken, allowing all nonlinear susceptibilities to be nonzero. This process is now commonly used in nonlinear microscopy[2,12–14] to observe transparent ob-

0146-9592/06/142214-3/$15.00

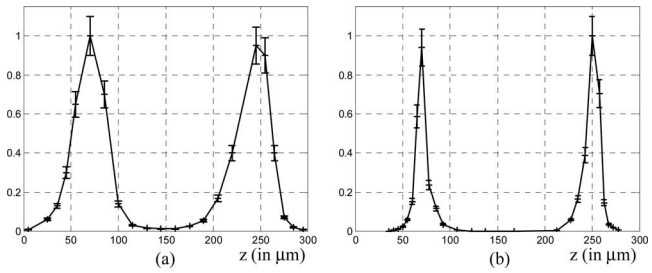

Fig. 1. THG signal as a function of axial distance z. (a) With uncorrected wavefront. (b) With corrected wavefront.

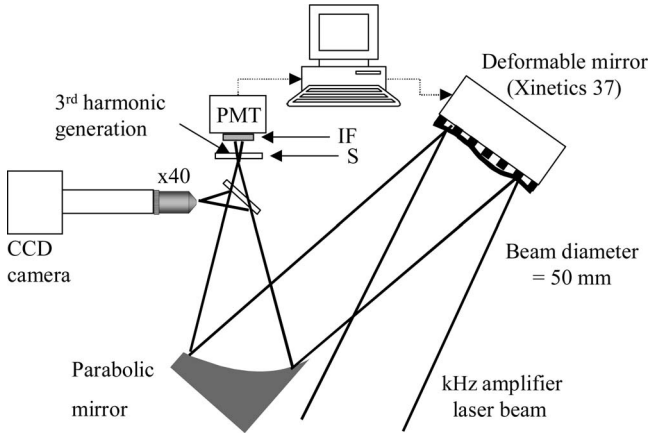

Fig. 2. Experimental setup for adaptive correction with THG signal generated at focus. IF, interference filter at 266 nm; PMT, photomultiplier tube; S, quartz slide.

jects through variations in nonlinear properties of the sample and to avoid the use of dye in biological samples. The measured THG signal we generated from a 180 μm thick quartz slide in the focus region is shown in Fig. 1 before and after wavefront correction. The two peaks corresponding to the air–quartz interfaces (front and back surfaces) are seen. Our aim was to use the front surface to generate the THG signal so that the slide itself does not introduce additional spherical aberration. The choice of this material was dictated by absorption at the third-harmonic wavelength of 266 nm; quartz transmits without significant attenuation at this wavelength. Other materials could be used but with restriction to optimization on the back surface.

The experimental setup is depicted in Fig. 2. The beam from a 1 kHz/0.5 mJ/40 fs Ti:sapphire laser amplifier is reflected off a 50 mm diameter, 37-actuator, deformable mirror. The beam is then focused by a parabolic mirror onto a 180 μm thick quartz microscope slide. The THG signal is directly measured with a photomultiplier tube placed as close as possible to the slide. A 10 nm FWHM interference filter centered at 266 nm blocks the fundamental beam. Two parabolic mirrors with different f-numbers, $f/2.85$ and $f/1.2$ (focal length 145 mm and 61 mm), are used. The longest focal length allows us to simultaneously obtain an image of the focal spot on a linear CCD by inserting a very thin slide (less than 200 μm) at 45° on the focusing beam. This enables us to track the effect of the wavefront correction made by the deformable mirror in real time.

To optimize the THG signal a genetic algorithm is used. It randomly generates a set, or a generation, of combinations of the actuator voltages and selects the optimum mirror correction that maximizes THG. The next generations inherit its mirror correction from those selected in the previous generation, allowing the algorithm to learn step by step (generation by generation) the optimal mirror correction. To avoid keeping a voltage that seems to increase the THG signal because of the fundamental laser energy fluctuation, a reference signal at 800 nm is simultaneously recorded with a photodiode to normalize the THG signal. The correction algorithm converges in approximately 20–30 generations, and the THG signal value is improved by an order of magnitude. Figure 3 shows convergence for both parabolic mirrors that were tested. The THG signal is obtained after reducing the fundamental beam energy with a waveplate, a cube polarizer, and some $\lambda/10$ neutral-density filters. This attenuation is needed to stay safely below the slide damage threshold and so that the photomultiplier tube does not saturate after the wavefront optimization. The damage threshold for the quartz slide we used was found to be around 100–150 nJ (for the $f/1.2$ parabolic mirror) of energy, after which the THG signal suddenly drops owing to the damage. The attenuation we use is different for each parabolic mirror, so the THG signal absolute values are not directly comparable. Consequently, these two curves are normalized.

Figure 4 shows the focal spot improvement for both parabolic mirrors. Many of the standard methods for assigning a quality factor to the focal spot are affected by difficulties similar to that of choosing an optimization signal. One quality factor is the Strehl ratio,[7] the ratio between the experimental peak focal intensity to that of the ideal spot. We calculate the ideal spot by taking the Fourier transform of the input beam profile, assuming a flat phase. The experimental intensity is obtained by taking an image of

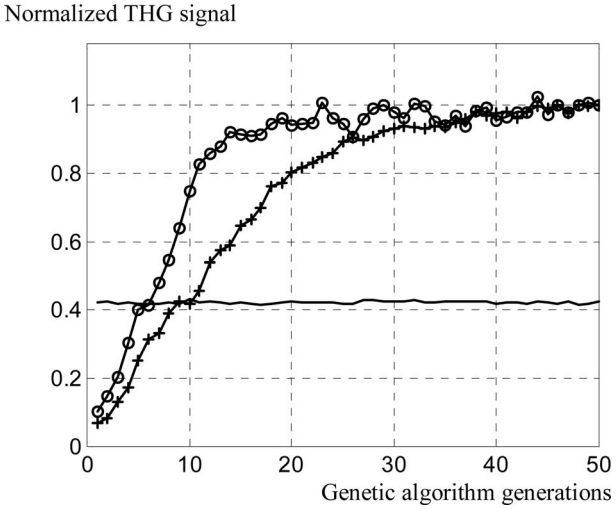

Fig. 3. Improvement of the THG signal as a function of algorithm generations. Circles, THG signal for $f/1.2$ parabola; crosses, THG signal for $f/2.85$ parabola; solid line, reference signal at 800 nm (in V).

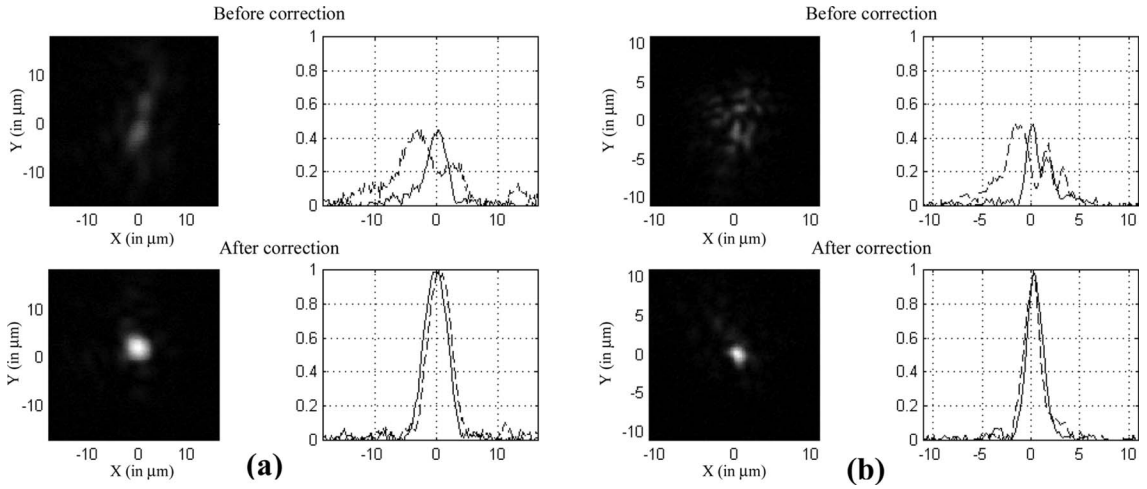

Fig. 4. (a) Experimental focal spot and lineouts of 800 nm beam before and after correction for the $f/2.85$ parabola. (b) Focal spot and lineouts of 800 nm beam before and after correction for the $f/1.2$ parabola.

the focal spot and normalizing it by integrating the image to obtain the total energy. The camera we used was only 8 bits, and the resulting error in this energy normalization could go either way. For the shorter-focal-length parabolic mirror ($f/1.2$, 0.4 NA), the Strehl ratio value is improved from 0.15 without correction to 0.71 after correction with the genetic algorithm. For this spot, the blurring of the spot by the objective would cause our measured Strehl ratio to be about 15% smaller than it should be. Since the objective is corrected for use with a cover glass, the measured Strehl ratio may also be slightly smaller. For the other parabolic mirror ($f/2.85$), the Strehl ratio is improved from 0.28 to 0.69 after correction. For the higher-NA parabola, the focal spot was recorded after removing the slide generating the THG signal while keeping the correcting voltages fixed.

Another way to check the effectiveness of the wavefront correction is to study the THG signal as a function of z, the position of the slide. It has been shown[12] that the FWHM of the THG peak is approximately equal to the Rayleigh range of the fundamental beam. From the plots of the THG signal as a function of z before and after correction (cf. Fig. 1), it is obvious that the wavefront correction reduces the FWHM of each peak. For this parabolic mirror (0.4 NA), the FWHM of the focal spot calculated by Fourier transform is 1.5 μm. By taking the corrected FWHM of the peak, the corresponding focal spot size is calculated (FWHM = 1.88 μm $\pm$ 0.1 μm) and is in excellent agreement with our measured focal spot shown in Fig. 4 (FWHM = 1.89 μm in the x and FWHM = 1.83 μm in the y direction).

In conclusion, we demonstrate how the third-harmonic signal generated at an air–dielectric interface can be used for wavefront correction of high-intensity lasers. Correction of a kilohertz, terawatt laser wavefront was accomplished by optimizing the THG signal via a genetic algorithm controlling the application of voltages on a 37-actuator deformable mirror. We believe this technique to be a simple, efficient, and inexpensive (no wavefront sensor needed) method for wavefront correction of high-intensity lasers, and it is well suited for tightly focused beam aberration correction. Notably, the principle of this method can also be applied to achieve high spatial resolution in multiphoton imaging microscopy.

This work was supported by the National Science Foundation under grant MRI PHY-0420357. The authors thank Seung-Whan Bahk for helpful discussions. T. A. Planchon's e-mail address is tplancho@mines.edu.

References

1. S.-W. Bahk, P. Rousseau, T. A. Planchon, V. Chvykov, G. Kalintchenko, A. Maksimchuk, G. A. Mourou, and V. Yanovsky, Opt. Lett. **29**, 2837 (2004).
2. J. A. Squier, D. N. Fittinghoff, C. P. J. Barty, K. R. Wilson, M. Muller, and G. J. Brakenhoff, Opt. Commun. **147**, 153 (1998).
3. Y. Barad, H. Eisenberg, M. Horowitz, and Y. Silberberg, Appl. Phys. Lett. **70**, 922 (1997).
4. M. A. A. Neil, M. J. Booth, and T. Wilson, Opt. Lett. **25**, 1083 (2000).
5. J.-C. Chanteloup, H. Baldis, A. Migus, G. Mourou, B. Loiseaux, and J.-P. Huignard, Opt. Lett. **23**, 475 (1998).
6. T. A. Planchon, J.-P. Rousseau, F. Burgy, G. Cheriaux, and J.-P. Chambaret, Opt. Commun. **252**, 222 (2005).
7. T. A. Planchon, P. Mercère, G. Cheriaux, and J.-P. Chambaret, Opt. Commun. **216**, 23 (2003).
8. O. Albert, H. Wang, D. Liu, Z. Chang, and G. Mourou, Opt. Lett. **25**, 1125 (2000).
9. P. Villoresi, S. Bonora, M. Pascolini, L. Poletto, G. Tondello, C. Vozzi, M. Nisoli, G. Sansone, S. Stagira, and S. De Silvestri, Opt. Lett. **29**, 207 (2004).
10. D. Yoshitomi, J. Nees, N. Miyamoto, T. Sekikawa, T. Kanai, G. Mourou, and S. Watanabe, Appl. Phys. B **78**, 275 (2004).
11. T. Y. F. Tsang, Phys. Rev. A **52**, 4116 (1995).
12. M. Muller, J. Squier, K. R. Wilson, and G. J. Brakenhoff, J. Microsc. **191**, 266 (1998).
13. J. A. Squier, M. Muller, and G. J. Brakenhoff, Opt. Express **3**, 315 (1998).
14. D. Yelin and Y. Silberberg, Opt. Express **5**, 169 (1999).